ARMY RESEARCH LABORATORY

# Statistical Studies of Mesoscale Forecast Models MM5 and WRF

by Teizi Henmi

ARL-TR-3329 September 2004

## NOTICES

### Disclaimers

**Army Research Laboratory**
White Sands Missile Range, NM 88002-5501

**ARL-TR-3329** **September 2004**

# Statistical Studies of Mesoscale Forecast Models MM5 and WRF

**Teizi Henmi**
*Computational and Information Sciences Directorate*

| **REPORT DOCUMENTATION PAGE** | *Form Approved* *OMB No. 0704-0188* |
|---|---|



| **1. REPORT DATE** *(DD-MM-YYYY)* | **2. REPORT TYPE** | **3. DATES COVERED (From - To)** |
|---|---|---|
| September 2004 | Final | Oct. 2003 – Sep. 2004 |

**4. TITLE AND SUBTITLE**
Statistical Studies of mesoscale Forecast Models MM5 and WRF

**5a. CONTRACT NUMBER**

**5b. GRANT NUMBER**

**5c. PROGRAM ELEMENT NUMBER**

**6. AUTHOR(S)**
Teizi Henmi

**5d. PROJECT NUMBER**

**5e. TASK NUMBER**

**5f. WORK UNIT NUMBER**

**7. PERFORMING ORGANIZATION NAME(S) AND ADDRESS(ES)**
U.S. Army Research Laboratory
Computational and Information Sciences Directorate
Battlefield Environment Division (ATTN: AMSRD-ARL-CI-EB)
White Sands Missile Range, NM 88002-5501

**8. PERFORMING ORGANIZATION REPORT NUMBER**
ARL-TR-3329

**9. SPONSORING/MONITORING AGENCY NAME(S) AND ADDRESS(ES)**
U.S. Army Research Laboratory
2800 Powder Mill Road
Adelphi, MD 20783-1145

**10. SPONSOR/MONITOR'S ACRONYM(S)**

**11. SPONSOR/MONITOR'S REPORT NUMBER(S)**
ARL-TR-3329

**12. DISTRIBUTION/AVAILABILITY STATEMENT**
Approved for public release; distribution is unlimited.

**13. SUPPLEMENTARY NOTES**

**14. ABSTRACT**
Two mesoscale weather forecasting models—the Mesoscale Model Version 5 (MM5) and the Weather Research and Forecast (WRF)—were statistically evaluated over two different geographical areas, Utah and western Texas. Using the 40-km Eta forecast data as input data, forecast calculations of both the models were carried out and the results were compared with surface observation data. Both models tended to over-forecast temperature and dew-point temperature, although the correlation coefficients between forecast and observations were fairly high. The statistical parameters for MM5 were slightly better than those for the WRF. For both MM5 and WRF, statistical parameters for wind vector components are inferior to those of temperature and dew-point temperature. The influences of different input data on the MM5 forecast fields were studied using the 40-km Eta and the Global Forecast System (GFS). For all surface meteorological parameters, the MM5 with the inputs from the 40-km Eta performed better than the MM5 with the GFS. The WRF forecasting over western Texas produced better statistical results than those over Utah, probably due to simpler terrain in western Texas as compared to Utah.

**15. SUBJECT TERMS**
Mesoscale models, Statistical evaluation, MM5, WRF.

| **16. SECURITY CLASSIFICATION OF:** | | | **17. LIMITATION OF ABSTRACT** | **18. NUMBER OF PAGES** | **19a. NAME OF RESPONSIBLE PERSON** |
|---|---|---|---|---|---|
| **a. REPORT** | **b. ABSTRACT** | **c. THIS PAGE** | SAR | 40 | Teizi Henmi |
| U | U | U | | | **19b. TELEPHONE NUMBER** (*Include area code*) (505) 678-3519 |

**Standard Form 298 (Rev. 8/98)**
Prescribed by ANSI Std. Z39.18

# Contents

## List of Figures

# List of Tables

INTENTIONALLY LEFT BLANK.

## Summary

Two mesoscale weather forecasting models—the Mesoscale Model Version 5 (MM5) and the Weather Research and Forecast (WRF)—were statistically evaluated over two different geographical areas, Utah and western Texas.

Using the 40-km Eta forecast data as input data, forecast calculations using both the MM5 and the WRF were carried out and the results were compared with surface observation data. Both models tended to over-forecast temperature and dew point temperature, although the correlation coefficients between forecast and observation were fairly high.

The statistical parameters for the MM5 were slightly better than for those for the WRF. For both the MM5 and the WRF, statistical parameters for wind vector components were inferior to those for temperature and dew-point temperature, though the values for the WRF were slightly better than the values for the MM5.

The influences of different input data on the MM5 forecast fields were studied using both the 40-km Eta and the Global Forecast System (GFS). For all surface meteorological parameters, the MM5 using the inputs from the 40-km Eta performed better than the MM5 using inputs from the GFS. The importance of input data to mesoscale models should be further studied.

Also, the WRF forecasting over the western Texas produced better statistical results than the forecasting over the Utah. This was probably due to the simpler terrain in western Texas, as compared to Utah.

# 1. Introduction

With advancements in both computer hardware and software (such as the availability of a parallel computer with distributed memory and Message Passage Interface), applications of non-hydrostatic meteorological models with many different physics options have become possible for operational use. Thus, it is important to evaluate how non-hydrostatic models perform over areas of complex terrain. Two such non-hydrostatic models—the Pennsylvania State University/National Center for Atmospheric Research (NCAR) Mesoscale Model Version 5 (MM5) and the Weather Research and Forecast (WRF) model, are the focus of this report.

In a statistical evaluation study comparing the MM5 and the Battlescale Forecast Model (BFM) (Henmi, 2003a) over a complex Utah terrain, the following results were obtained:

- No significant statistical differences in forecast skills were found between the MM5, domain 3 (7.5-km grid resolution), and the MM5, domain 4 (2.5-km grid resolution). Similarly, the forecast skills of two BFM (5- and 2.5-km grid resolutions) were also found to be statistically similar. Forecast results did not significantly improve for either model even when the grid resolutions were reduced.
- Both the MM5 and the BFM produced more accurate forecast results for surface temperature than for dew-point temperature and wind vector components.
- For all of the surface meteorological parameters of temperature, dew-point temperature, and wind vector, the MM5 demonstrated statistically better forecasting skills than the BFM.
- Both the MM5 and the BFM produced better forecasting statistics during the period of April to June 2002 than during the period of January to March 2002.

The forecasting skills of the MM5's surface meteorological parameters were statistically evaluated using three different planetary boundary layer (PBL) parameterization schemes— the Medium Range Forecast model (MRF), the Blackadar, and the Eta PBL (Henmi, 2003b). The MM5's surface temperature forecasting skills were found to be similar when using each of three different schemes; all were slightly positively biased. However, for dew-point temperature, the MM5 using the Eta PBL parameterization scheme produced significantly positively biased results during the local daylight hours. For wind speed and direction, each scheme produced similar statistical results: the correlation coefficient (CC) for wind speed was between 0.3 and 0.5, the mean absolute difference (AD) was slightly smaller than 2.0 m/sec, and the mean wind direction difference (MWDDF) was between 50º and 60º.

A comparison study of the forecast skills of the MM5 between two domains (with a 15- and 5-km grid resolution) (Henmi, 2003b) showed that, for temperature and dew-point temperature, the model domain with the 5-km increment produced slightly better forecasting results than the model domain with the 15-km increment. Also, for wind speed and the direction and vector components, $u$ and $v$, the model domain with the 5-km grid resolution produced better wind forecasts than the one using the 15-km grid resolution.

The MM5 produced statistically better forecasting results for all surface meteorological parameters when it used initialization and time-dependent lateral boundary data from the Aviation Forecast Model (AVN) rather than from the Navy Operational Global Atmospheric Prediction System (NOGAPS). Initialization and lateral boundary value data are essential for producing reliable forecasting results.

In the continuing efforts of mesoscale model evaluation, the objectives of this present study are as follows:

- To compare the WRF and MM5 models. For this study, initialization and time-dependent lateral conditions were provided by the forecast data of the 40-km Eta produced by the National Center of Environmental Prediction (NCEP).
- To study the influences of different initialization and lateral-boundary condition data on the MM5 forecast, by using data provided by the 40-km Eta and by the Global Forecasting System (GFS), using a 1° grid resolution. (Both datasets are from the NCEP.)
- To examine the influences of different geographical and topographical areas on statistical parameters, using the model domains in Utah and western Texas.

For the present study, a triple-nested MM5 was used, and since a WRF with nesting capability was not available when the study was started, version 1.3 of the WRF (which does not have a nesting capability) was used.

Section 2 briefly describes the MM5 and the WRF. The model domains, input data, and statistical parameters used in this study are mentioned in section 3. Section 4 shows the results of study, and section 5 presents the conclusions.

## 2. The MM5 and the WRF

### 2.1 The MM5

The distributed-memory version of the MM5 was used. The source code of the MM5 was obtained from the MM5 home page (2001).

The MM5 is based on non-hydrostatic dynamics and features multiple-nest capabilities and many physics options. Details of this modeling system can be found in Dudhia (1993), Grell et al. (1994), and Warner et al. (1992).

For the present study, the following physics options were employed:

- PBL. The PBL technique used was that of the MRF model of the NCEP by Hong and Pan (1996).
- Precipitation parameterization. This study applied a simple treatment of cloud microphysics based on Dudhia (1989), in which both ice and liquid phases are permitted for cloud and precipitation, but mixed phases are not permitted.
- Cumulus parameterization. For this aspect, the study used Grell's scheme, which is based on rate of destabilization, or quasi-equilibrium; features a simple single-cloud scheme with

updraft and downdraft fluxes; and uses compensating motion to determine the heating and moistening profile (1994).

- Radiation parameterization. Dudhia's scheme, in which long-wave and short-wave radiation interact with the clear atmosphere, clouds, precipitation, and the ground (1989), was used.
- Ground temperature scheme. This study utilizes a multilayer, soil temperature model.

## 2.2 The WRF

The WRF is a weather forecasting system with fully compressible, non-hydrostatic equations (unlike the MM5, which is based on incompressible, non-hydrostatic equations). Therefore, the WRF can be used to simulate atmospheric phenomena, including acoustic and gravity waves. Details of the WRF are available on the WRF home page (2004).

As with the MM5, the WRF can use a number of different physics options. For the present study, the following physics options were used:

- PBL. A new scheme, known as the Yonsei University PBL, was used. It has an explicit representation of entrainment at the PBL top, which is derived from large eddy modeling. This scheme partially corrects the problem of too much entrainment in the early phase of PBL growth and also adds non-local momentum mixing to provide a realistic wind profile in the PBL (Dudhia, 2004).
- Precipitation parameterization. The WRF Single-Moment 3-class was used (Hong, Dudhia, and Chen, 2004). In this scheme, ice crystal number concentration is dependent on ice mass content rather than temperature, giving realistic ice crystal concentrations and size that are compatible with the fall speeds.
- Cumulus parameterization. The modified version of the Kain-Fritch scheme (1990, 1993) was selected. This scheme utilizes a simple cloud model with moist updrafts, including the effects of detrainment, entrainment, and cloud microphysics. A minimum entrainment rate is imposed to suppress widespread convection in marginally unstable, relatively dry environments. Shallow (non-precipitating) convection is allowed for any updraft that does not reach minimum cloud depth for precipitating clouds; this cloud depth varies as a function of cloud-base temperature. In this version, the entrainment rate is allowed to vary as a function of low-level convergence.
- Radiation parameterization. For long-wave radiation, the rapid radiative transfer model (RRTM) (Mlawer et al., 1997) was used. The RRTM is a spectral-band scheme that uses preset tables to accurately represent long wave processes due to water vapor, ozone, $CO_2$ , and trace gases (if present) as well as accounts for cloud optical depth. For short-wave radiation, a scheme based on Dudhia (1989) was used.
- Ground temperature scheme. The five-layer, soil temperature model used in the MM5 was used for the WRF as well.

In June 2004, the WRF version 2, with one-way and two-way multiple nesting capabilities, was released. However, for the present study, the WRF version 1.3 was used (which was released in 2003); this version does not possess a nesting capability.

## 3. Model Domains, Input Data, and Statistical Parameters

### 3.1 Model Domains

The MM5 triple-nested computational grids, depicted in figure 1, were used for the Utah model domains. All three computational domains have a mesh size of 55 by 55 grid points and grid resolutions of 45, 15, and 5 km for domains 1, 2, and 3, respectively. For the present study, only the forecast fields for domain 3 are compared with the observed data.

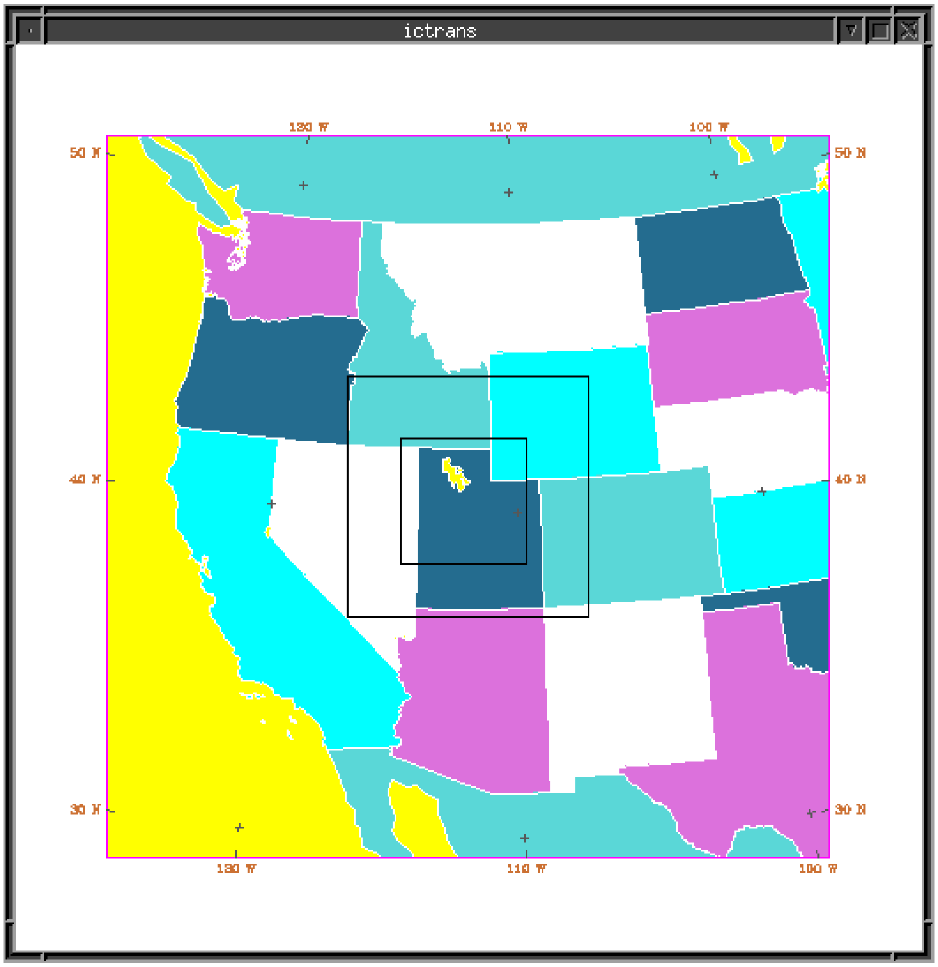


Figure 1. Geographical extents of the three MM5 computational domains in Utah.

Figure 2 shows the terrain contours of the MM5, covering domains 2 and 3. The locations of the GFS grid points are marked using the "#" symbol and the 40-km ETA grid points are marked using the "*" symbol.

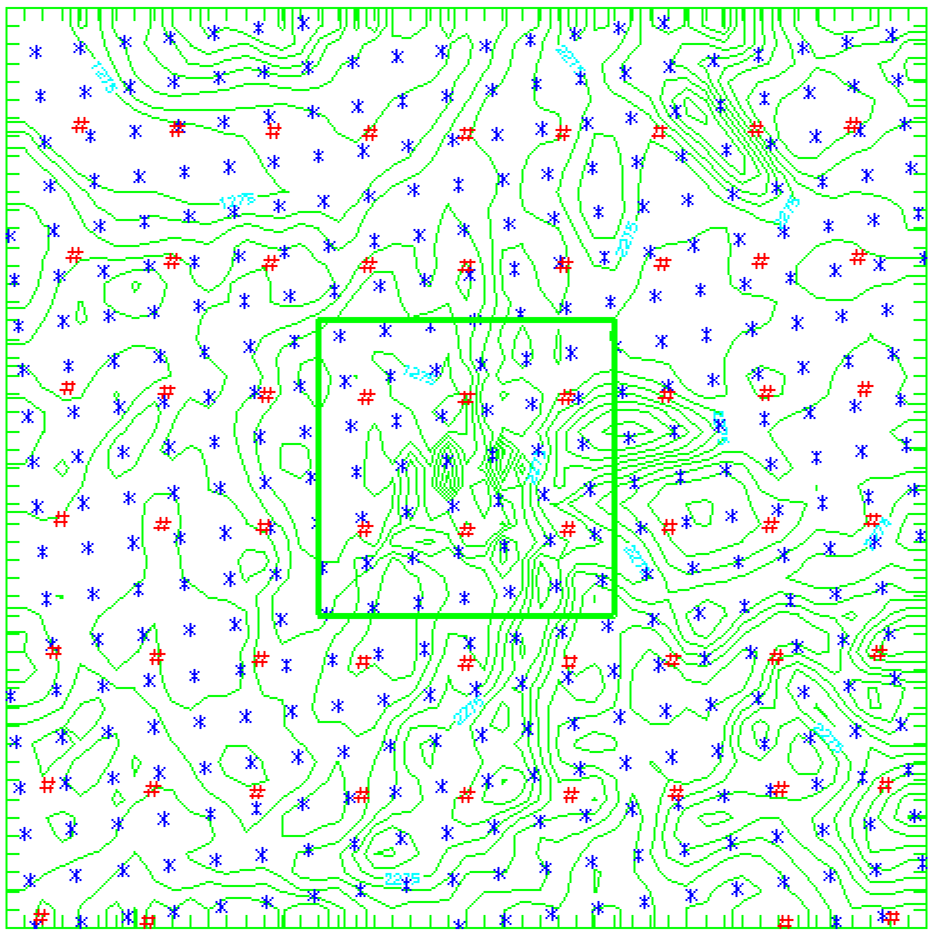


Figure 2. Terrain contours of the MM5 domains 2 and 3 for Utah.

The WRF used the model domain shown in figure 3. The domain was centered at lat. 40.5ºN and long. 112.5ºW, with a grid point number of 52 by 52 and a grid resolution of 5 km. In figure 3, the "*" symbol represents the location of the 40-km Eta grid point and the letter "S" represents the location of the surface observation sites used for the comparison study. The size and geographical location of this model domain are similar to that of the MM5, domain 3, as shown in figure 1.

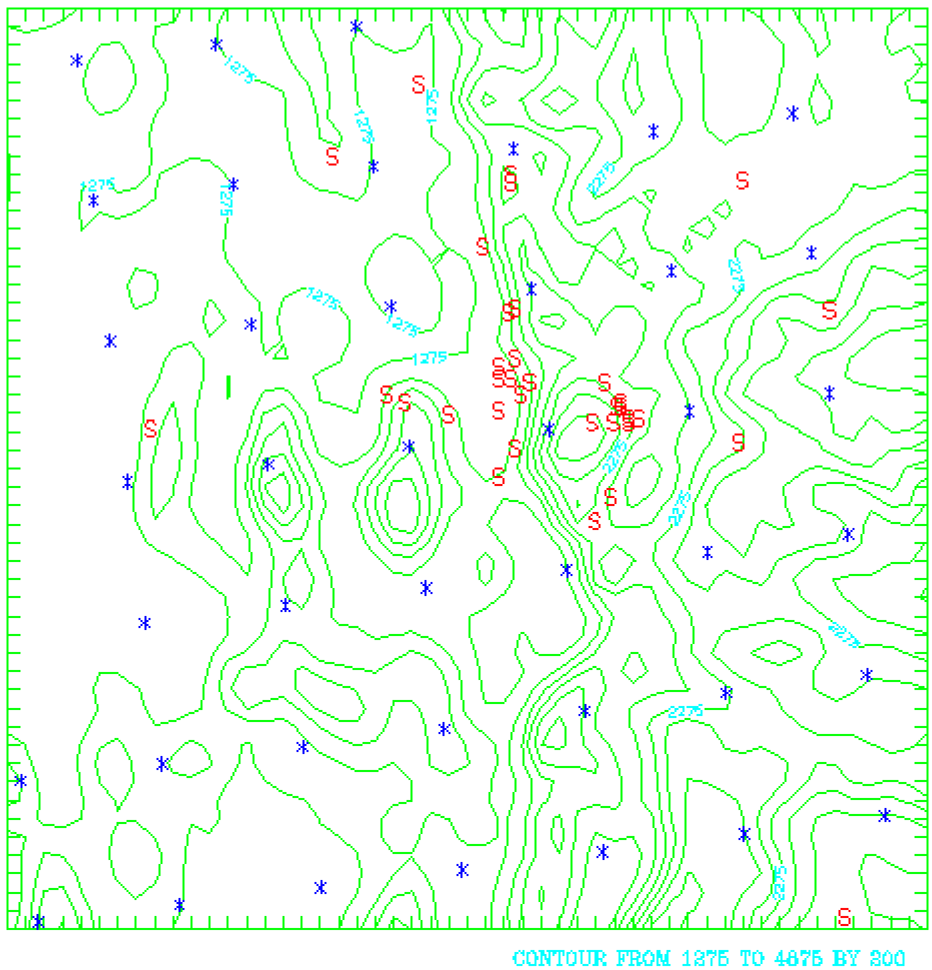


Figure 3. Terrain contours of the WRF model domain in Utah, using a 52-by-52 grid and a 5-km grid resolution.

The model domain of the western Texas area for the WRF is shown in figure 4. As can be seen, this domain is flatter and simpler than the terrain in the Utah domain. In figure 4, the "*" symbol represents the locations of the 40-km Eta grid point and the letter "S" represents the location of the Texas Tech University (TTU) Mesonet observation site. The domain is centered at 33.82ºN and 101.82ºW and has 52 by 52 grid points and a 5-km grid resolution.

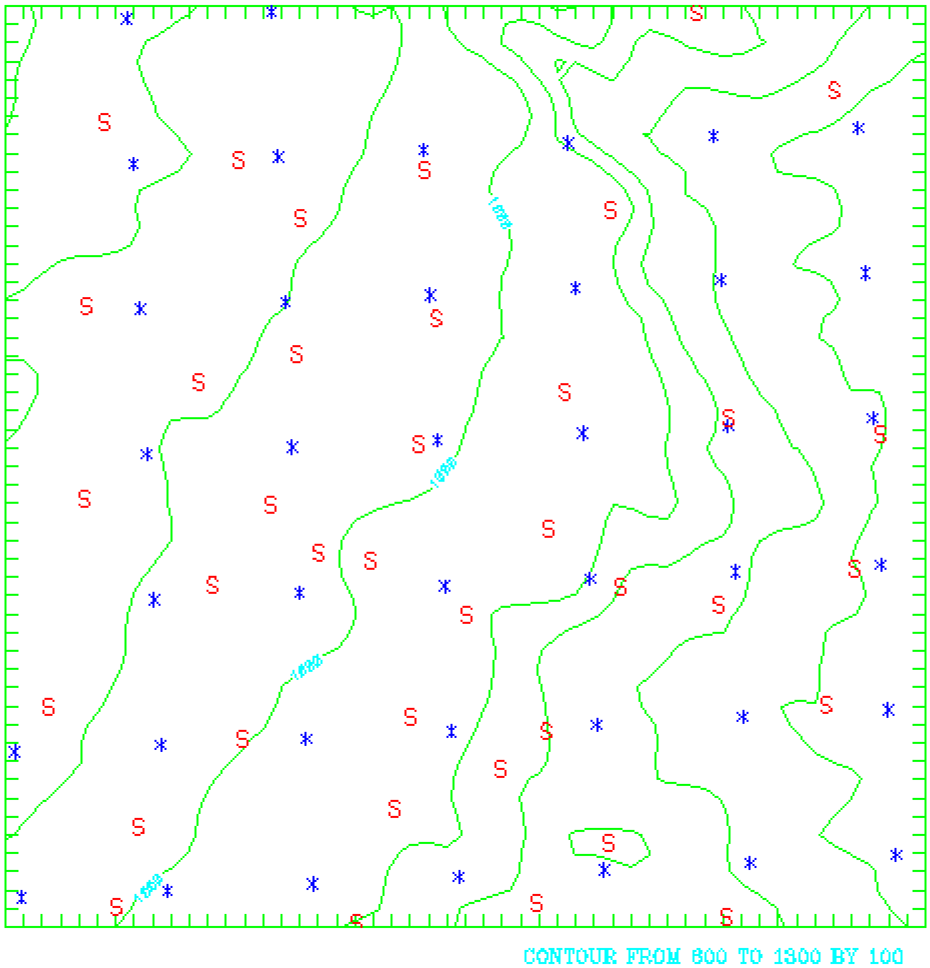


Figure 4. Terrain contours of the western Texas model domain for the WRF.

NOTE: The "*" symbol represents the 40-km Eta grid points; the letter "S" represents the Texas Tech. University Mesonet observation sites.

## 3.2 Input Data

The 40-km Eta forecast data is used for initialization and time-dependent lateral condition. This dataset was used for the comparison study of the MM5 and the WRF. The data is freely available from the NCEP FTP site: ftpprd.ncep.gov.

GFS data, with a 1º grid resolution, was also used to examine the influences of different input data on the MM5 forecasting over the Utah domain. This dataset can also be obtained from the NCEP FTP site.

Both the MM5 and the WRF were initialized at 1800 universal time coordinated (UTC) and were run for 30 hours. Comparisons between model output data and observation data were made every hour, starting from 0000 UTC.

Surface observation data for the Utah area is freely available from the University of Utah MesoWest Cooperative. A MesoWest data file, `total.dat`, contains data, in 15-min intervals, for a 24-h period for the western United States.

Data for the western Texas domain was obtained from the TTU FTP sites, which contain monthly files for each station.

A daily data file, containing data only for the even hours of a 24-h period (starting at 0000 UTC), was created from the above datasets for each domain area.

### 3.3 Statistical Parameters

The following statistical parameters were calculated for comparisons between the forecast and observation data:

- Mean difference (MD)
- Mean AD
- Root mean square error (RMSE)
- Root mean square vector error (RMSVE)
- Correlation coefficient (CC)
- Mean wind direction difference (MWDDF)

The details of these parameters are described in Henmi (2003a).

## 4. Results

A comparison study of the MM5 and the WRF over the Utah model domains was done using 29 daily forecast and surface observation conducted between March 30 and April 27, 2004.

The 40-km Eta forecast data was used for this study. Forecast calculations of the WRF over the western Texas domain were also conducted using the 40-km Eta forecast data during the same time period.

To study the influences of different initialization and lateral boundary condition data (the 40-km Eta versus the GFS), a 15-day period between April 16 through April 30, 2004 was selected, and the forecast data of the MM5, domain 3, was compared with the surface observation data.

### 4.1 Comparison study of the MM5 and WRF

#### 4.1.1 Statistical Parameters for the Entire Dataset

Statistical parameters between forecast data and surface observation data were calculated covering the entire datasets for 29 days, between March 30 2004 and April 27 2004. The

statistical parameters for the MM5 and WRF (given in tables 1 and 2, respectively) were based on about 24,000 data pairs.

Table 1. Statistical parameters between the MM5, domain 3, forecast data and surface observed data for the period of March 30 through April 27, 2004.

| | MD | AD | RMSE | CC |
|---|---|---|---|---|
| **Temperature (ºC)** | 1.0 | 2.5 | 3.2 | 0.87 |
| **Dew-point temperature (ºC)** | -0.2 | 3.2 | 4.2 | 0.63 |
| **Wind speed (m/sec)** | 1.0 | 2.2 | 2.8 | 0.35 |
| **Wind vector x-component (m/sec)** | -0.1 | 1.9 | 2.9 | 0.45 |
| **Wind vector y-component (m/sec)** | 0.9 | 2.3 | 3.1 | 0.55 |

NOTE: RMSVE = 4.2 (m/sec), MWDDF = 46º

Table 2. Statistical parameters between the WRF forecast data and surface observed data for the period of March 30 through April 27, 2004.

| | MD | AD | RMSE | CC |
|---|---|---|---|---|
| **Temperature (ºC)** | 0.7 | 2.9 | 3.8 | 0.81 |
| **Dew -point temperature (ºC)** | 2.8 | 3.7 | 5.1 | 0.64 |
| **Wind speed (m/sec)** | 0.5 | 1.8 | 2.4 | 0.41 |
| **Wind vector x-component (m/sec)** | -0.2 | 1.8 | 2.7 | 0.44 |
| **Wind vector y-component (m/sec)** | 0.4 | 2.0 | 2.8 | 0.54 |

NOTE: RMSVE = 3.8 m/sec, MWDDF = 47º

The scatter diagrams of temperature between the forecast data and observation for the MM5 and the WRF are shown in figures 5 and 6, respectively.

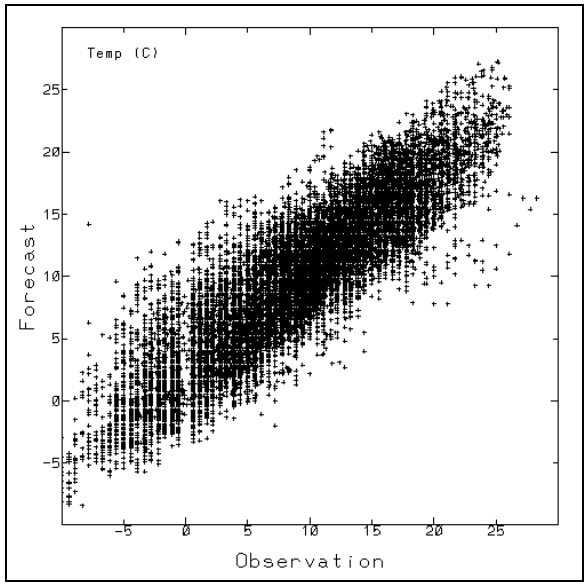


Figure 5. Scatter diagrams of temperature between forecast data and observation, for the MM5.

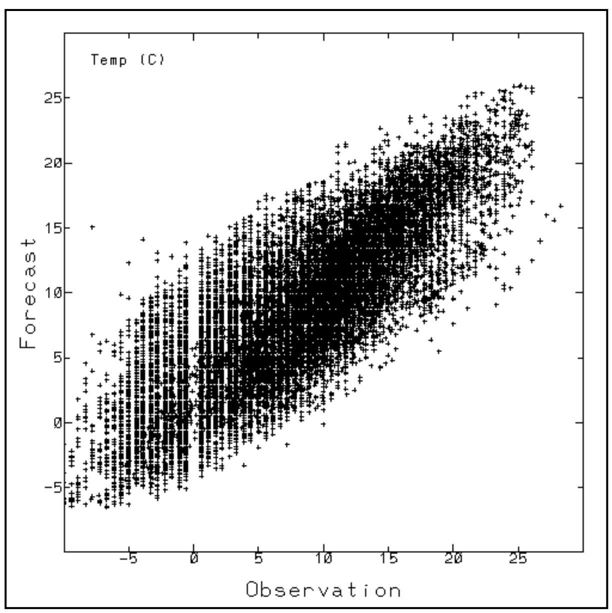


Figure 6. Same as figure 5, except for the WRF.

Scatter diagrams of dew-point temperature between forecast and observation data for the MM5 and the WRF are given in figures 7 and 8, respectively.

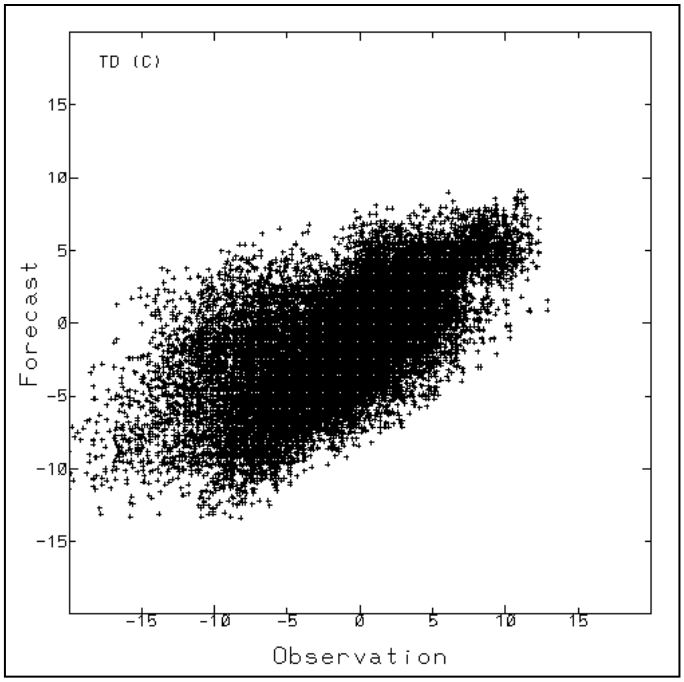


Figure 7. Scatter diagram of dew-point temperature between forecast and observation for the MM5.

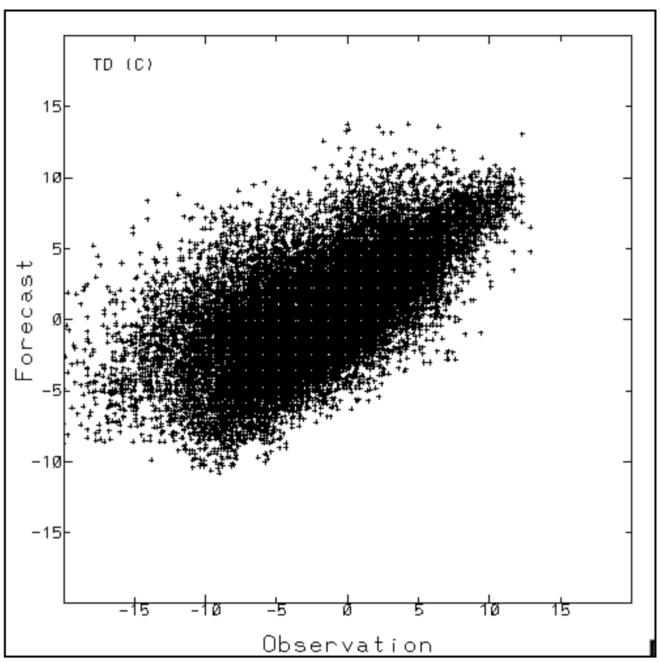


Figure 8. Same as figure 7, except for the WRF.

Scatter diagrams for wind speed between forecast and observation data for the MM5 and the WRF are shown in figure 9 and 10, respectively.

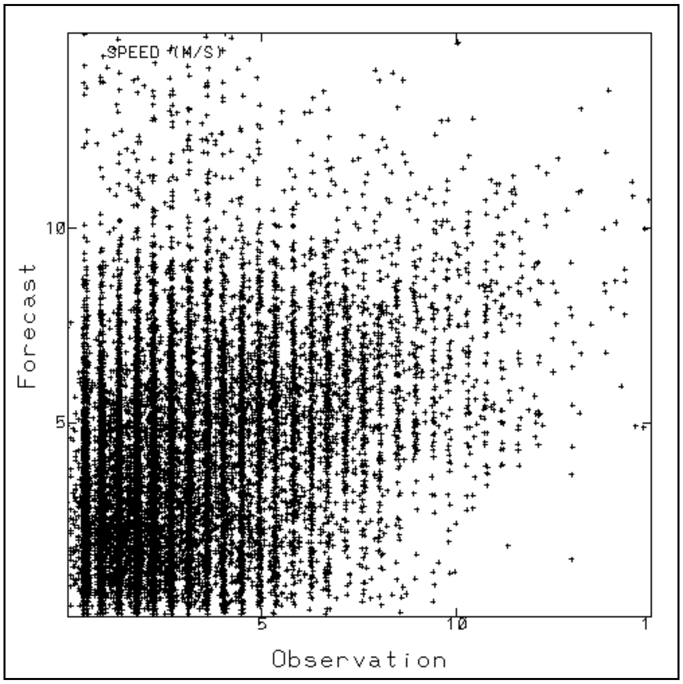


Figure 9. Scatter diagram of wind speed between forecast and observation, for the MM5.

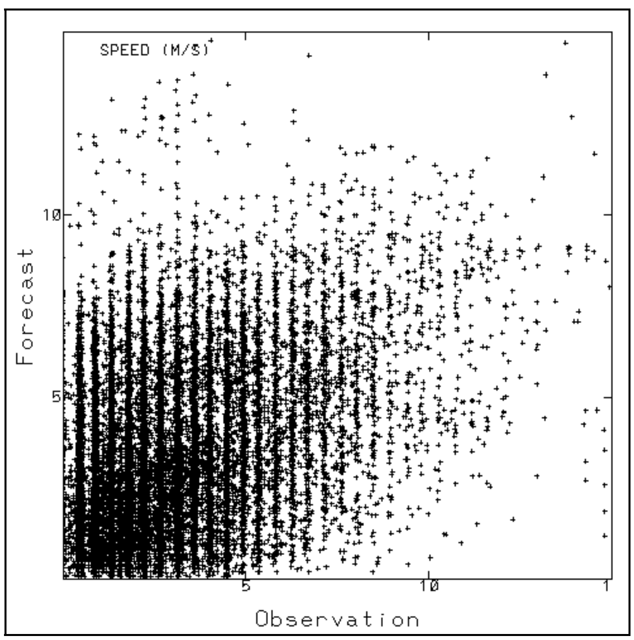


Figure 10. Same as figure 9, except for the WRF.

#### 4.1.2 Time Series of the Statistical Parameters (MD, CC, and AD)

The statistical parameters, MD, CC, and AD, (as mentioned in section 3.3) are calculated at each forecast hour using all available data for the 29-day period. In the following figures 11-14, time series of the MD, CC, and AD for the MM5 and the WRF are plotted using different colors (pink for the MM5 and black for the WRF).

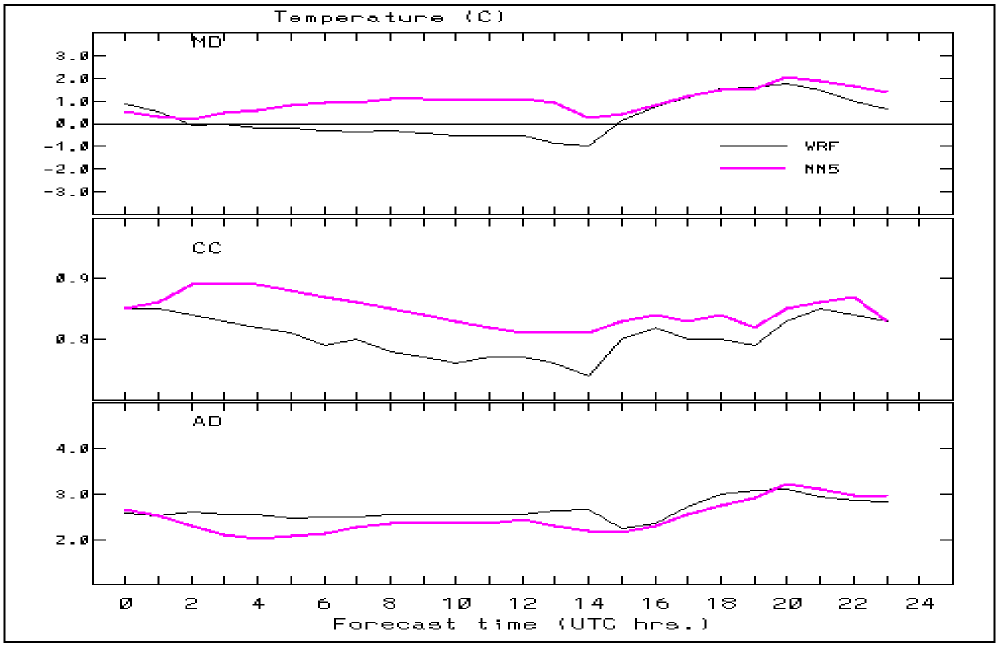


Figure 11. Time series of MD, CC, and AD for temperature.

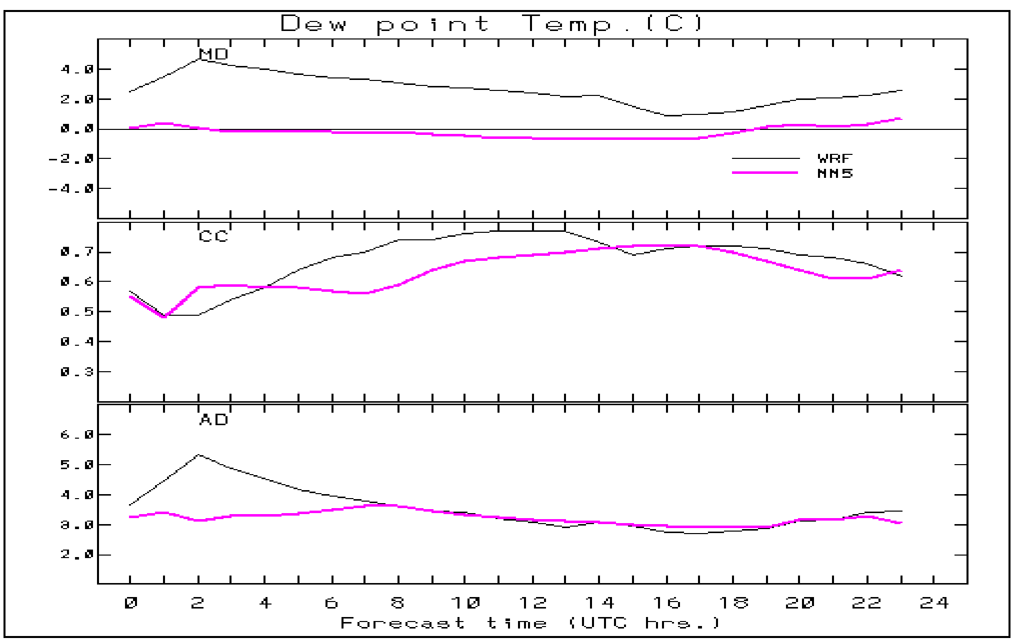


Figure 12. Same as figure 11, except for dew-point temperature.

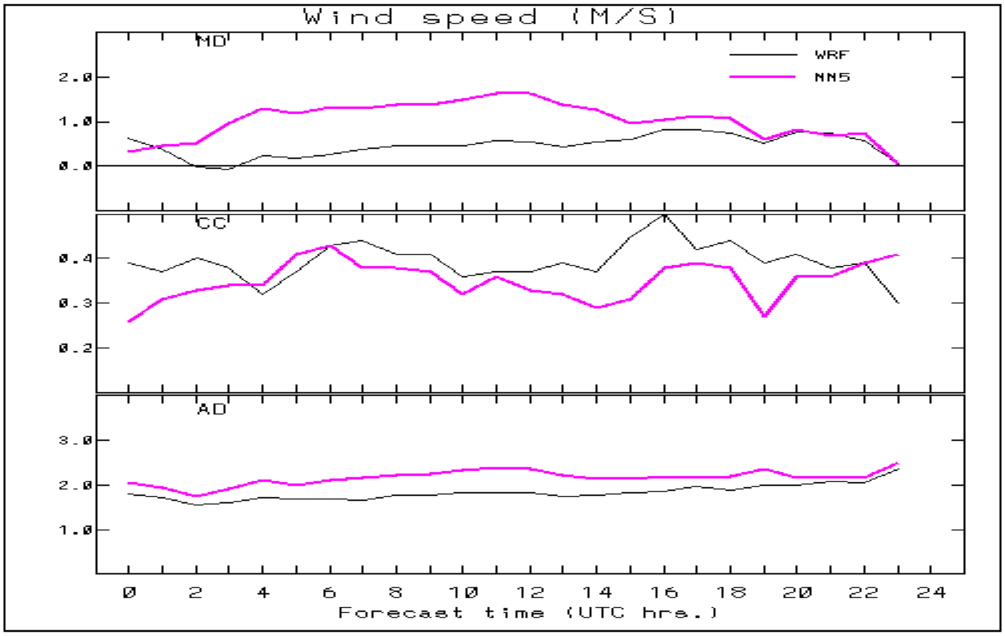


Figure 13. Same as figure 11, except for wind speed.

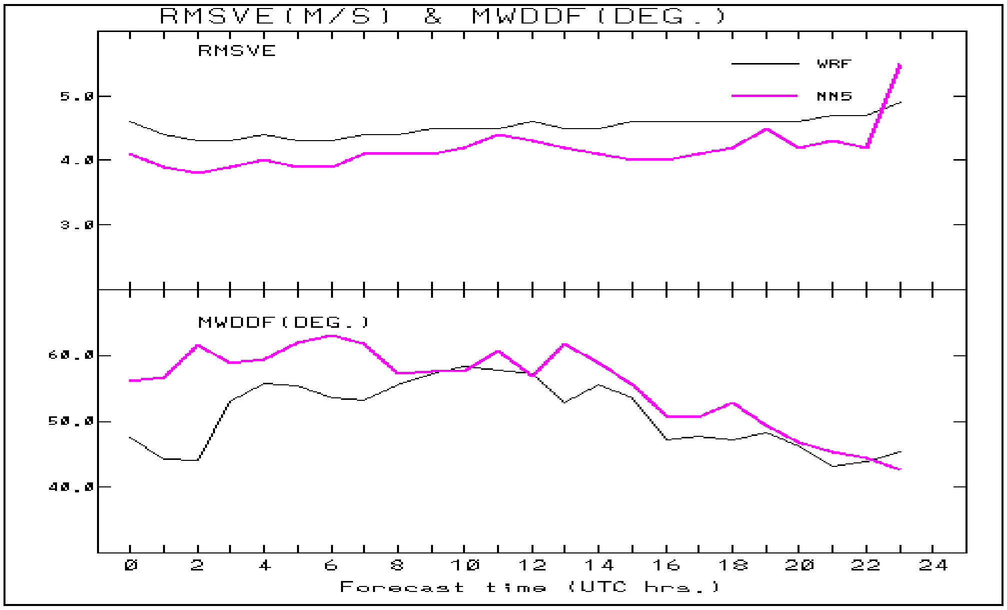


Figure 14. Time series of RMSVE and MWDDF.

From tables 1 and 2 and figures 5 through 14, the following can be inferred:

1. For temperature forecast, the MM5 produced better statistical results, although both models simulated temperature well, producing a CC greater than 0.8 and an AD between 2 ºC and 3 ºC.

2. As can be seen from the MD values, the WRF tended to over-forecast dew-point temperature significantly, yielding an MD of 2.8 for the entire dataset, in contrast to the MD of -0.17 for the MM5 (see tabs. 1 and 3).

3. For wind speed, the MM5 showed a tendency to produce greater values than the observed values throughout the 24-h period (see fig. 13). As seen in both models, the statistical parameters relating to wind vector indicate that forecasting surface wind by mesoscale models is difficult and challenging over such complex terrains as seen in the Utah domain.

### 4.2 Study of Different Input Data on the MM5 Forecast

In a previous study on the influences of different global forecast models (AVN and NOGAPS) as input data to the MM5 (Henmi, 2003 b), it was shown that an MM5 using the AVN data as initialization and boundary value data produces, for statistical parameters (MD, CC, RMSE, and AD), better forecasting results of surface meteorological parameters than an MM5 using NOGAPS data. The time series lines of statistical parameters for both AVN and NOGAPS are almost parallel throughout the 24-h forecast period. This was especially significant for temperature and dew-point temperature, indicating the differences between AVN and NOGAPS data were systematic, but not random, over the model domain of Utah.

This study looked at the influences of the GFS and the 40-km Eta model as input data to the MM5. The locations of grid points of both models over the MM5 domain of Utah are shown in figure 2. In the MM5, domain 3, there are 6 GFS grid points in contrast to 39 Eta grid points.

Table 3 shows the statistical parameters between the MM5 forecast and the surface observation data using the 40-km Eta forecast data as initialization and time-dependent lateral condition. These statistical parameters were obtained using 10,528 data during 15-day period in April 2004.

Table 3. Statistical parameters between the MM5 forecast and surface observation data using the 40-km Eta as input data.

| | MD | AD | RMSE | CC |
|---|---|---|---|---|
| **Temperature (ºC)** | 1.6 | 2.6 | 3.4 | 0.88 |
| **Dew-point temperature (ºC)** | -1.0 | 3.0 | 3.9 | 0.54 |
| **Wind speed (m/sec)** | 0.9 | 2.1 | 2.8 | 0.31 |
| **Wind vector x-component (m/sec)** | -0.1 | 1.9 | 2.9 | 0.41 |
| **Wind vector y-component (m/sec)** | 0.6 | 2.2 | 2.9 | 0.54 |

NOTE: RMSVE = 4.1 m/sec, MWDDF = 46º

The statistical parameters obtained using the GFS data as input data are shown in table 4; the data were obtained for the same period as the 40-km Eta data.

Table 4. Same as table 3, except for the GFS as input data.

| | MD | AD | RMSE | CC |
|---|---|---|---|---|
| **Temperature (ºC)** | 1.6 | 3.1 | 4.1 | 0.82 |
| **Dew-point temperature (ºC)** | -0.8 | 3.1 | 4.0 | 0.46 |
| **Wind speed (m/sec)** | 1.4 | 2.4 | 3.1 | 0.26 |
| **Wind vector x-component (m/sec)** | -0.2 | 2.2 | 3.2 | 0.38 |
| **Wind vector y-component (m/sec)** | 0.0 | 2.5 | 3.3 | 0.46 |

NOTE: RMSVE = 4.52 m/sec, MWDDF = 45.4º

Figures 15 through 18 are time series of the statistical parameters (MD, CC, and AD). In these figures, different colors—pink for the 40-km Eta, and black for the GFS—are used to plot the data.

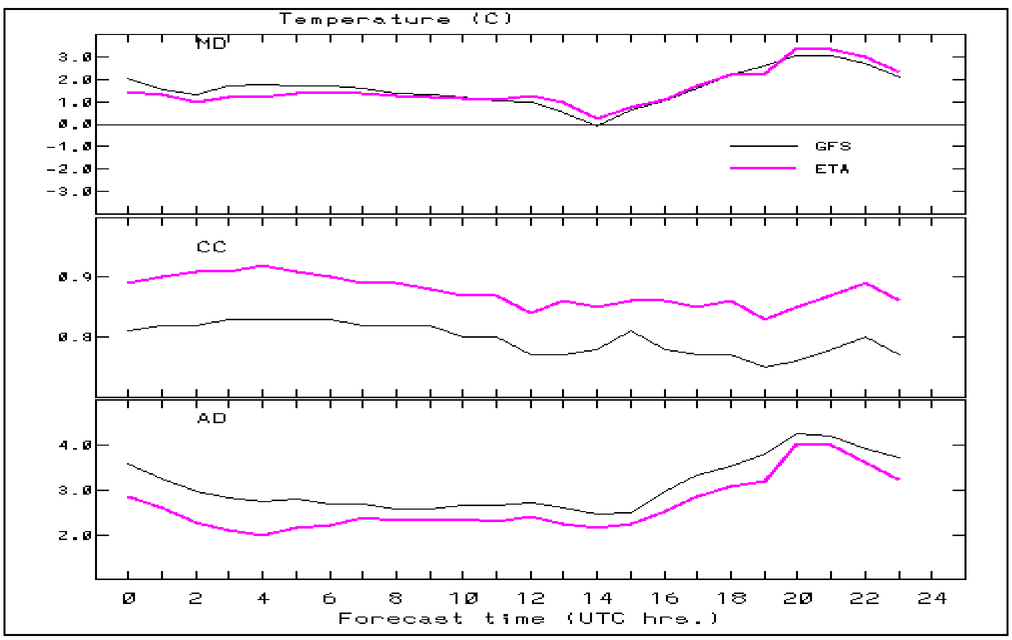


Figure 15. Time series of statistical parameters (MD, CC, and AD) for temperature between the MM5 forecast and surface observation data.

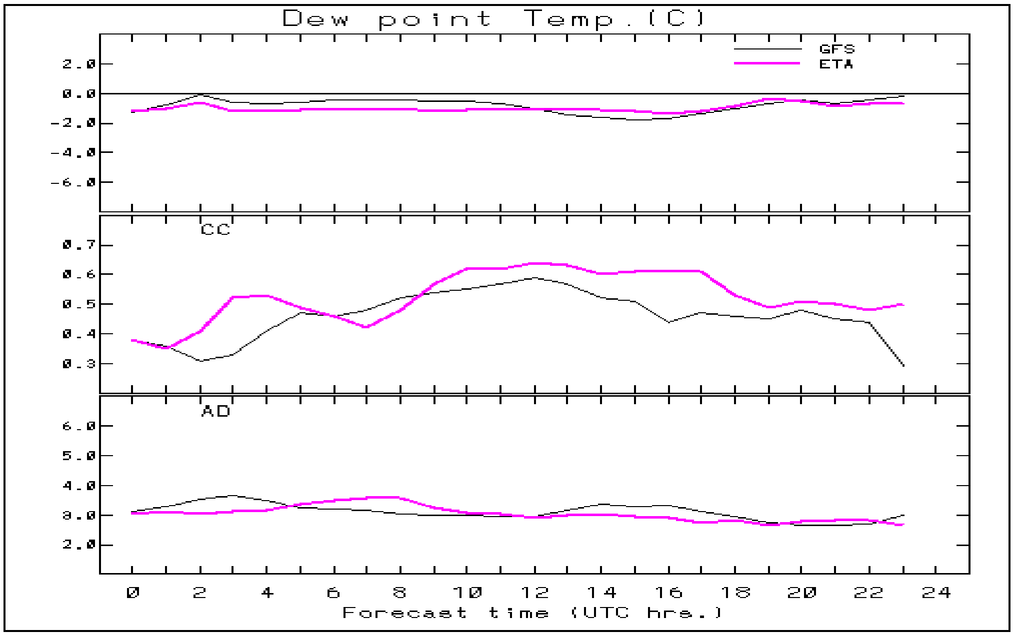


Figure 16. Same as figure 15, except for dew-point temperature.

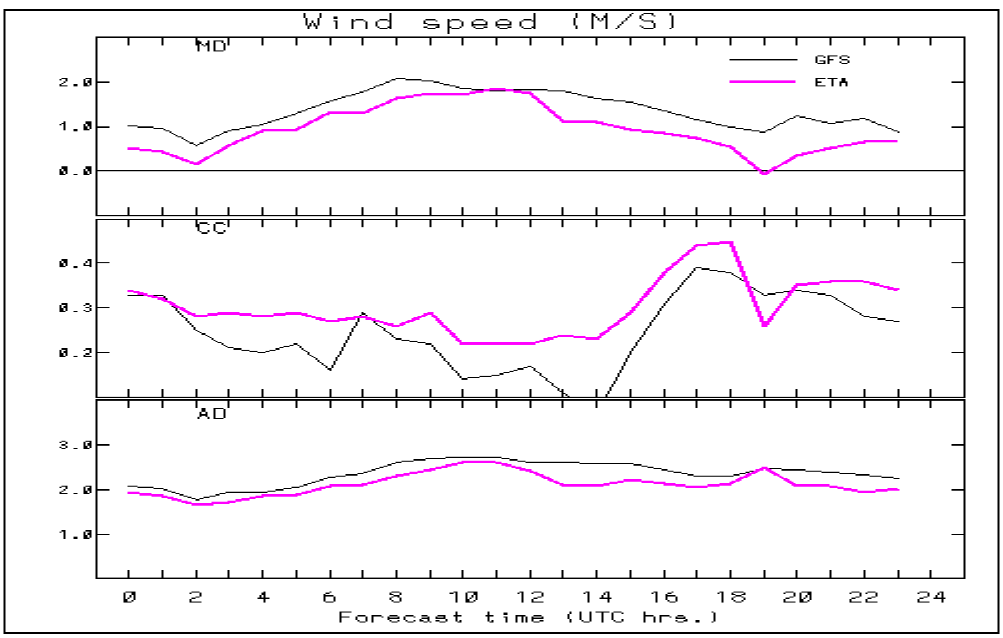


Figure 17. Same as figure 15, except for wind speed.

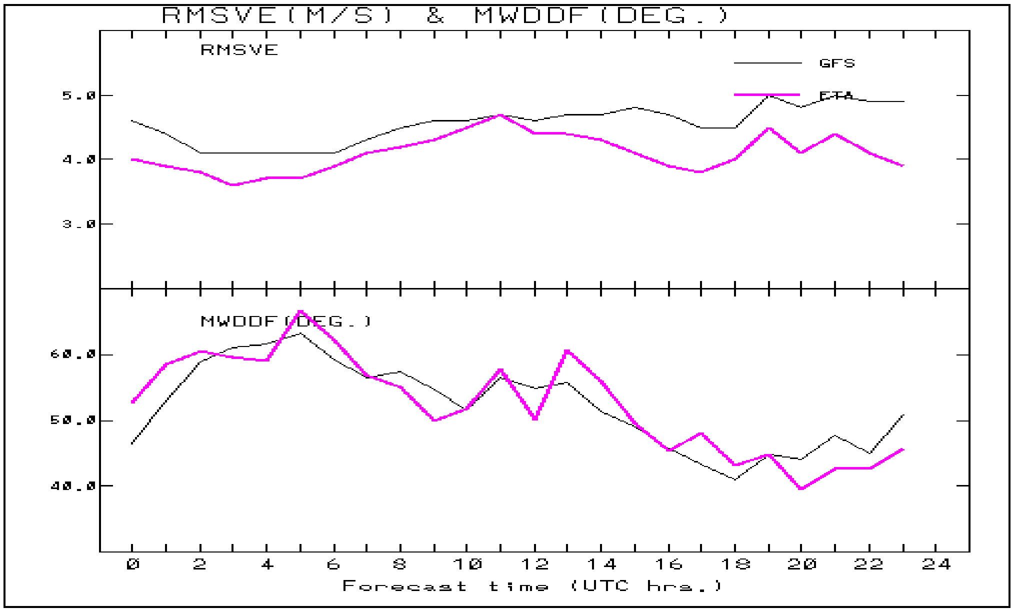


Figure 18. Time series of RMSVE and MWDDF.

As seen in tables 3 and 4 and figures 15 through 18, the MM5 produces statistically better forecasting results for all surface meteorological parameters when using the initialization and lateral boundary data from the 40-km Eta rather than using the data from the GFS.

In a previous study (Henmi, 2003b), for the same model domain during 11-day period in February 2003, the MM5 produced statistically better forecasting results for all surface meteorological parameters when it used the initialization and lateral boundary data from the GFS rather than the data from the NOGAPS.

Thus, it is important to choose appropriate forecast data from a large-scale forecast model as input to mesoscale models such as the MM5 and WRF.

### 4.3 Study of the WRF Forecasting Over the Domain of the Western Texas

The terrain contour plot of the western Texas used for the WRF forecast calculation is shown in figure 4. The area can be characterized by a gradual sloping from west to east, and it is flatter and simpler than the terrain in the Utah domain (shown in fig. 3). It should be also noted that in this model domain, the surface observation sites were distributed much more evenly than those in the Utah domain.

The statistical results given in this section were based on about 18,000 data points from twenty 24-h forecast calculations during April 2004.

The statistical parameters (MD, AD, RMSE, and CC), contrasted between the WRF forecast and observation data, are given in table 5.

Table 5. Statistical parameters between the WRF forecast and observation data over the western Texas domain.

| | MD | AD | RMSE | CC |
|---|---|---|---|---|
| **Temperature (ºC)** | 2.5 | 2.7 | 3.7 | 0.91 |
| **Dew Point Temperature (ºC)** | 2.9 | 3.2 | 4.5 | 0.77 |
| **Wind Speed (m/sec)** | -1.2 | 1.9 | 2.6 | 0.49 |
| **Wind Vector x-component (m/sec)** | 0.0 | 1.8 | 2.5 | 0.72 |
| **Wind Vector y-component (m/sec)** | 0.7 | 2.2 | 3.2 | 0.78 |

NOTE: RMSVE = 4.1 (m/sec), MWDDF = 33º

Scatter diagrams between forecast and observation data for temperature, dew-point temperature, and wind speed are displayed in figures 19, 20, and 21, respectively.

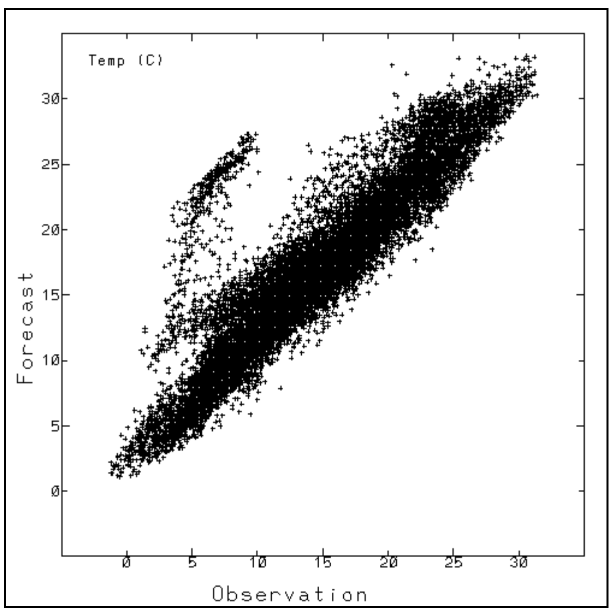


Figure 19. Scatter diagram between the WRF forecast and observation data over the western Texas, for temperature.

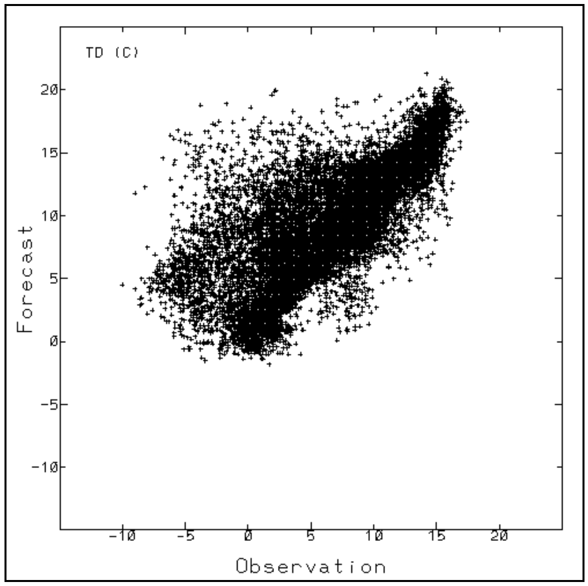


Figure 20. Same as figure 19, except for dew-point temperature.

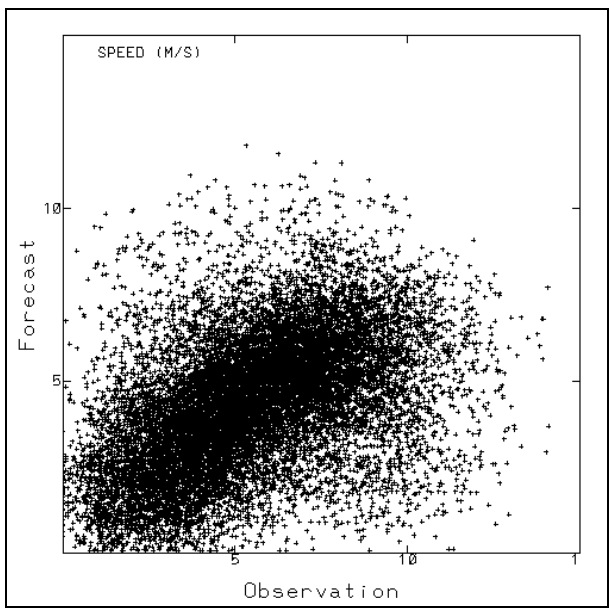


Figure 21. Same as figure 19, except for wind speed.

The significant over-forecasting of temperatures, seen at the upper-left part of figure 19, is caused by the failures of the WRF (and the 40-km Eta) to simulate the passage of a cold front over the area on April 10, 2004.

Time series of the statistical parameters are shown in figures 22-25.

In figure 23, which shows the dew-point temperature statistics, a significantly small CC and large MD and AD are seen at the early hours of forecast, with peaks at 0100 UTC. Examination of data reveals that these large deviations are caused by large values of dew-point temperature

for several of the forecast days. In this study, dew-point temperature at the 2-m level is calculated as follows, using Tetan's formula (Yamada, 1989):

$$P_2 = P_0\left(\frac{\theta_2}{T_2}\right)^{\kappa} \tag{1}$$

$$A = \log\left(\frac{P_2 \times Q_2}{3.8002}\right) \tag{2}$$

$$TD_2 = \frac{35.86 \times A - 17.27 \times 273.16}{A - 17.27} \tag{3}$$

where

$P_2$ : pressure at 2-m level (mbar),

$P_0$ : standard pressure (1000 mbar),

$\theta_2$ : potential temperature at 2-m level (ºK),

$T_2$ : temperature at 2-m level (ºK),

$Q_2$ : mixing ratio at 2-m level (g/kg), and

$TD_2$ : dew-point temperature (ºK).

$$\kappa = R_d / C_p \tag{4}$$

where

$R_d$ : gas constant for dry air

$C_p$ : specific heat at constant pressure

The WRF output file contains $\theta_2$, $T_2$, and $Q_2$. Further study is needed to examine which parameter(s) caused the large dew-point temperature deviations from the observation data.

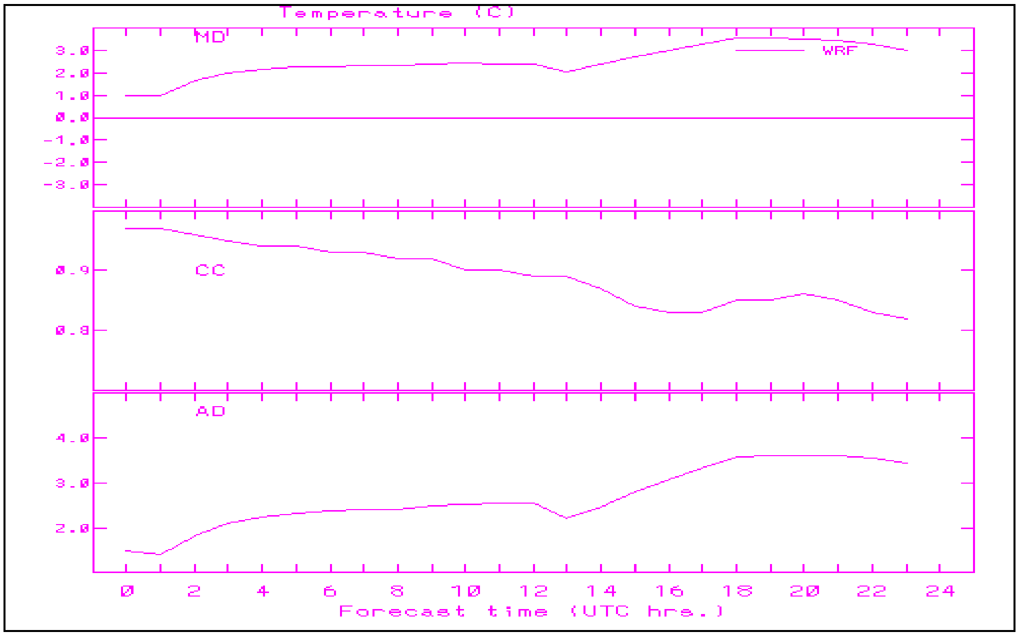


Figure 22. Time series of statistical parameters (MD, CC, and AD) between the WRF forecast and observation data over the western Texas domain for temperature.

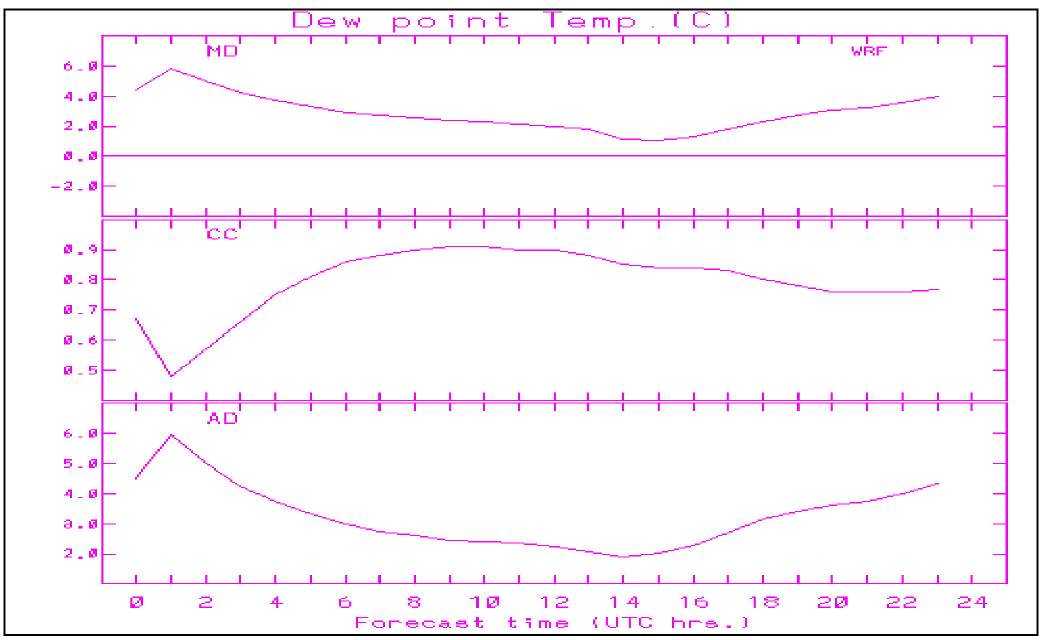


Figure 23. Same as figure 22, except for dew-point temperature.

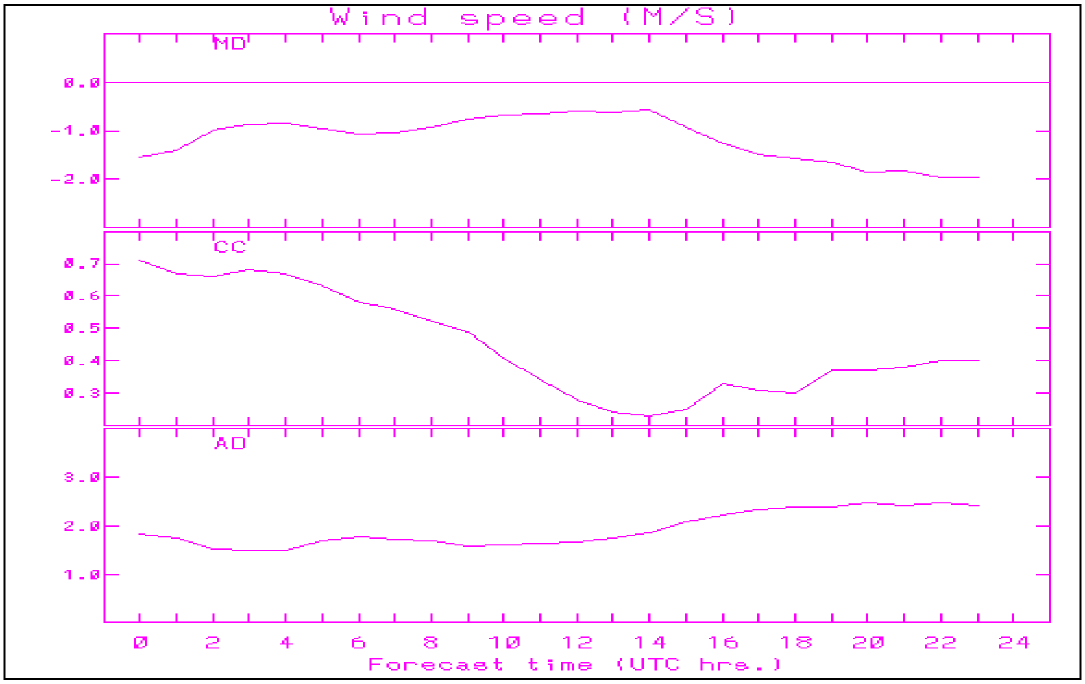


Figure 24. Same as figure 22, except for wind speed.

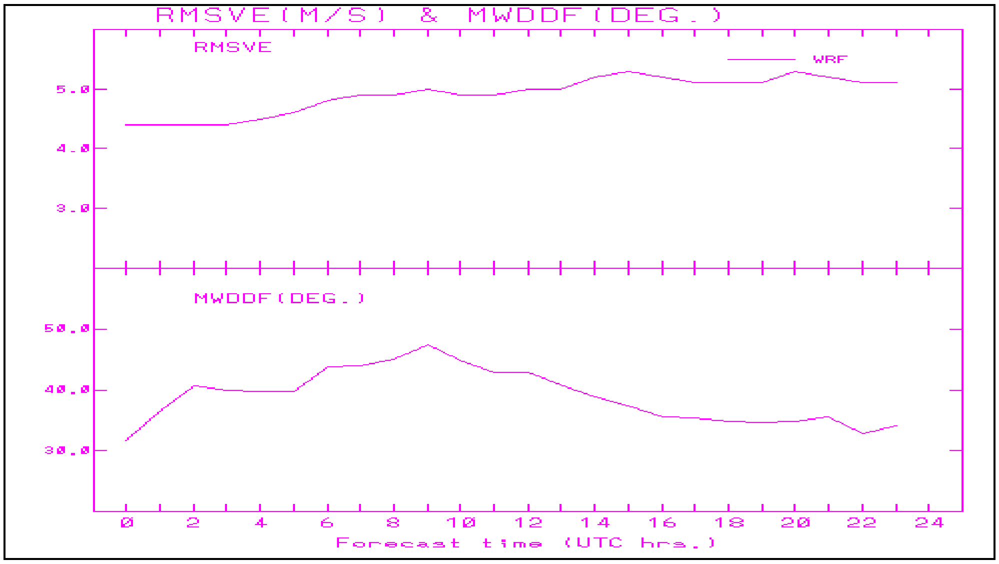


Figure 25. Time series of RMSVE and MWDDF for the WRF forecast and observation data over the western Texas.

The tables, scatter diagrams, and time series of the statistical parameters reveal that the WRF over-forecasted temperature and dew-point temperature over the western Texas domain during the period of April 2004. Similarly, the WRF overestimated temperature and dew-point temperature over the Utah domain. Thus, it is necessary to examine whether or not the over-forecasting of temperature and dew-point temperature is due to the 40-km Eta forecast data used as initialization and time-dependent lateral boundary condition.

Let us compare the statistics of the WRF forecast over the Utah domain and the western Texas domain, although such a comparison is qualitative:

- The statistical parameters over the western Texas domain are superior to those over the Utah domain (see tabs. 2 and 5).
- From the comparisons of scatter diagrams (figs. 6 and 19, figs. 8 and 20, and figs. 10 and 21), the correlations between the WRF forecast and observation are better over the western Texas domain than over the Utah domain.

The better statistical results may have been a result of the simpler terrain features and better quality-controlled observation data over the western Texas domain.

## 5. Conclusions

The forecasting skills of surface meteorological parameters of two mesoscale models, MM5 and WRF, were statistically evaluated over two different geographical areas, Utah and western Texas. Both areas have networks for conducting surface meteorological observation.

A triple-nested MM5, with grid resolutions of 45, 15, and 5 km for domains 1, 2, and 3, respectively, was used over the Utah area. For the present study, only the forecast fields for domain 3 were compared with the observed data.

The WRF version 1.3, which does not have multiple-nesting capability, was used with a 52-by-52 grid size and a 5-km grid resolution. The model was applied to the model domains of both Utah and western Texas. Over the Utah domain, the WRF domain covered an area similar to the MM5, domain 3.

Using the 45-km Eta forecast data as input data, forecast calculations of both the MM5 and the WRF were carried out, and the results were compared with surface observation data. Both models tended to over-forecast temperature and dew-point temperature, although the correlation coefficients between forecast and observation were fairly high.

The statistical parameters for MM5 were slightly better than those for the WRF. For both the MM5 and the WRF, the statistical parameters for wind vector components were inferior to those of temperature and dew-point temperature, although the WRF values were slightly better than the MM5 values.

It is important to do comparative studies of the MM5 and WRF with similar model domain configurations. With recent arrival of the WRF version 2, which has a multiple nesting capability, such studies have now become possible.

Also studied were the influences of different input data for initialization and time-dependent lateral condition on the MM5 forecast fields. To do this, data from the 45-km Eta and the GFS were used and the results compared. For all surface meteorological parameters, the MM5 using the 45-km Eta performed better than the MM5 using the GFS. The importance of input data to mesoscale models should be further studied using other large-scale model outputs, such as a GFS with 0.5° grid resolution and a 45-km Eta.

Also, the WRF forecasting over the western Texas domain produced better statistical results than forecasting over the Utah domain, probably due to simpler and more monotonous terrain found in the western Texas as compared to Utah. Furthermore, the surface observation data network over the western Texas appears to provide more appropriate datasets for mesoscale model evaluation. In the future, this Mesonet dataset will be used for mesoscale model evaluation study.

## References


Dudhia, J. A. Numerical Study of Convection Observed During the Winter Monsoon Experiment Using a Mesoscale Two-Dimensional Model. *J. of Atmos. Sci.* **1989**, *46*, 3077–3107.

Dudhia, J. A. Non-hydrostatic Version of the Penn State-NCAR Mesoscale Model: Validation Tests and the Simulation of an Atlantic Cyclone and Cold Front. *Mon. Wea. Rev.* **1993**, *121*, 1493–1513.

Dudhia, J. *The Weather Research and Forecast Model Version 2.0: Physics Update*, WRF/MM5 Summer Workshop, Extended Abstract, National Center for Atmospheric Research, 2004.

Grell, G.A.; Dudhia,J.; Stauffer, D. R. *A Description of the Fifth Generation Penn State/NCAR Mesoscale Model (MM5)*; 398+STR; National Center for Atmospheric Research, 1994.

Henmi, T. *Evaluation Study of Mesoscale Models MM5 and BFM Over the Model Domains of Utah Using Surface Meteorological Data by MesoWest*; ARL-TR-2928; U.S. Army Research Laboratory: White Sands Missile Range, NM, 2003a.

Henmi, T. *Forecasting Skills of Mesoscale Model MM5 of Surface Meteorological Parameters*; ARL-TR-3113; U.S. Army Research Laboratory: White Sands Missile Range, NM, 2003b.

Hong, S. Y.; Dudhia, J.; Chen, S.H. A Revised Approach to Ice Microphysical Processes for the Bulk Parameterization of Cloud and Precipitation. *Monthly Weather Rev.* **2004**, *132*, 103.

Kain, J.S.; Fritch, J.M. A On-dimensional Entraining/Dtraining Plume Model and Its Application in Convective Parameterization. *J. of Atmos. Sci.* **1990**, *47*, 2784–2802.

Kain, J.S.; Fritch, J.M. *Convective Parameterization for Mesoscale Models: The Kain-Fritch Scheme*. The Representation of Cumulus Convection in Numerical Models. K.A. Emanuel and D. J. Raymond, eds.; American Meteorological Society, 1993, 246 pp.

Mlawer, E.J.; Taubman, S.J.; Brown, P.D.; Iacono, M.J.; Clough, S.A. Radiative Transfer for Inhomogeneous Atmosphere: RRTM, a Validated Correlated-k Model for the Long-wave. *J. of Geophysical Res.* **1997**, *102* (D14), 16663–11182.

Warner, T.T.; Kuo, Y. H.; Doyle, J. D.; Dudhia, J.; Stauffer, D. R.; Seaman, N. L. Non-Hydrostatic, Mesobeta-Scale Real-Data Simulation with the Penn State University/National Center for Atmospheric Research Mesoscale Model. *Met. and Atmos. Physics* **1992**, *49*, 209–227.

## Acronyms

| | |
|---|---|
| AD | absolute difference |
| AVN | Aviation Forecast Model |
| BFM | Battlescale Forecast Model |
| CC | correlation coefficient |
| GFS | Global Forecast System |
| MD | mean difference |
| MM5 | Mesoscale Model Version 5 |
| MRF | Medium Range Forecast model |
| MWDDF | mean wind direction difference |
| NCAR | National Center for Atmospheric Research |
| NCEP | National Center for Environmental Prediction |
| NOGAPS | Navy Operational Global Atmospheric Prediction System |
| PBL | planetary boundary layer |
| RMSE | root mean square error |
| RMSVE | root mean square vector error |
| RRTM | rapid radiative transfer model |
| TTU | Texas Tech University |
| UTC | universal time coordinated |
| WRF | Weather Research and Forecast model |

## Distribution List

| | Copies |
|---|---|
| NASA SPACE FLT CTR<br>ENVIRONMENTS GROUP<br>CODE ED 44<br>HUNTSVILLE AL 35812 | 1 |
| US ARMY MISSILE CMND<br>REDSTONE SCI INFO CTR<br>AMSMI RD CS R DOC<br>REDSTONE ARSENAL AL 35898-5241 | 1 |
| PACIFIC MISSILE TEST CTR<br>GEOPHYSICS DIV<br>ATTN CODE 3250<br>POINT MUGU CA 93042-5000 | 1 |
| ATMOSPHERIC PROPAGATION BRANCH<br>SPAWARSYSCEN SAN DIEGO D858<br>49170 PROPAGATION PATH<br>SAN DIEGO CA 92152-7385 | 1 |
| METEOROLOGIST IN CHARGE<br>KWAJALEIN MISSILE RANGE<br>PO BOX 67<br>APO SAN FRANCISCO CA 96555 | 1 |
| NCAR LIBRARY SERIALS<br>NATL CTR FOR ATMOS RSCH<br>PO BOX 3000<br>BOULDER CO 80307-3000 | 1 |
| HQ DEPT OF ARMY<br>DAMI POB<br>WEATHER TEAM<br>1000 ARMY PENTAGON ROOM 2E383<br>WASHINGTON DC 20310-1067 | 1 |
| HQ AFWA/DNX<br>106 PEACEKEEPER DR STE 2N3<br>OFFUTT AFB NE 68113-4039 | 1 |

| | Copies |
|---|---|
| AFRL/VSBL<br>29 RANDOLPH RD<br>HANSCOM AFB MA 01731 | 1 |
| ARL CHEMICAL BIOLOGY<br>NUC EFFECTS DIV<br>AMSRD ARL SL CO<br>APG MD 21010-5423 | 1 |
| US ARMY RESEARCH LAB<br>AMSRD ARL CI OK TL<br>2800 POWDER MILL ROAD<br>ADELPHI MD 20783-1197 | 1 |
| US ARMY RESEARCH LAB<br>AMSRD ARL SE EE<br>ATTN DR SZTANKAY<br>2800 POWDER MILL ROAD<br>ADELPHI MD 20783-1145 | 1 |
| US ARMY RESEARCH LAB<br>AMSRD ARL CI<br>ATTN J GANTT<br>2800 POWDER MILL ROAD<br>ADELPHI MD 20783-1197 | 1 |
| US ARMY RSRC OFC<br>ATTN AMSRD ARL RO EN<br>PO BOX 12211<br>RTP NC 27009 | 1 |
| US ARMY CECRL<br>CRREL GP<br>ATTN DR DETSCH<br>HANOVER NH 03755-1290 | 1 |
| ARMY DUGWAY PROVING GRD<br>STEDP MT M<br>ATTN MR BOWERS<br>DUGWAY UT 84022-5000 | 1 |
| USAF ROME LAB TECH<br>CORRIDOR W STE 262 RL SUL<br>26 ELECTR PKWY BLD 106<br>GRIFFISS AFB ROME NY 13441-4514 | 1 |

| | Copies |
|---|---|
| US ARMY<br>FIELD ARTILLERY SCHOOL<br>ATSF TSM TA<br>FT SILL OK 73503-5600 | 1 |
| NAVAL SURFACE WEAPONS CTR<br>CODE G63<br>DAHLGREN VA 22448-5000 | 1 |
| US ARMY OEC<br>CSTE EFS<br>PARK CENTER IV<br>4501 FORD AVE<br>ALEXANDRIA VA 22302-1458 | 1 |
| US ARMY CORPS OF ENGRS<br>ENGR TOPOGRAPHICS LAB<br>ATTN CETEC TR G PF KRAUSE<br>ALEXANDRIA VA 2215-3864 | 1 |
| US ARMY TOPO ENGR CTR<br>CETEC ZC 1<br>FT BELVOIR VA 22060-5546 | 1 |
| SCI AND TECHNOLOGY<br>10 BASIL SAWYER DRIVE<br>HAMPTON VA 23666-1293 | 1 |
| USATRADOC<br>ATCD FA<br>FT MONROE VA 23651-5170 | 1 |
| US ARMY TRADOC<br>ANALYSIS CMND<br>ATRC WSS R<br>WSMR NM 88002-5502 | 1 |
| US ARMY RESEARCH LAB<br>AMSRD ARL CI E<br>COMP & INFO SCI DIR<br>WSMR NM 88002-5501 | 1 |

| | Copies |
|---|---|
| WSMR TECH LIBRARY BR<br>STEWS IM IT<br>WSMR NM 88002 | 1 |
| US ARMY CECOM<br>INFORMATION & INTELLIGENCE<br>WARFARE DIRECTORATE<br>ATTN AMSEL RD IW IP<br>FORT MONMOUTH NJ 07703-5211 | 1 |
| NAVAL RESEARCH LABORATORY<br>MARINE METEOROLOGY DIVISION<br>7 GRACE HOPPER AVENUE STOP 2<br>MONTEREY CA 93943-5502 | 1 |
| US ARMY RESEARCH LABORATORY<br>ATTN SFAE C3T IE II<br>ROBERT DICKENSHIED<br>WSMR NM 88002 | 1 |
| ADMNSTR<br>DEFENSE TECHL INFO CTR<br>ATTN DTIC OCP<br>8725 JOHN J KINGMAN RD STE 0944<br>FT BELVOIR VA 22060-6218 | 1 |
| US ARMY RESEARCH LABORATORY<br>ATTN IMNE AD IM DR<br>MAIL & RECORDS MGMT<br>ADELPHI MD 20783-1197 | 1 |
| US ARMY RESEARCH LAB<br>AMSRD ARL CI OK TL<br>2800 POWDER MILL ROAD<br>ADELPHI MD 20783-1197 | 2 |
| TOTAL | 34 |